Molecular Catalysis 498 (2020) 111263

Contents lists available at ScienceDirect

Molecular Catalysis

journal homepage: www.journals.elsevier.com/molecular-catalysis

A mineralogically-inspired silver–bismuth hybrid material: Structure, stability and application for catalytic benzyl alcohol dehydrogenations under continuous flow conditions

Rebeka Mészáros [a], Sándor B. Ötvös [b,c,*], Gábor Varga [d,e], Éva Böszörményi [d,e], Marianna Kocsis [d,e], Krisztina Karádi [e], Zoltán Kónya [f,g], Ákos Kukovecz [f], István Pálinkó [d,e,**], Ferenc Fülöp [a,b,*]

[a] Institute of Pharmaceutical Chemistry, University of Szeged, Eötvös u. 6, Szeged, H-6720 Hungary
[b] MTA-SZTE Stereochemistry Research Group, Hungarian Academy of Sciences, Eötvös u. 6, Szeged, H-6720 Hungary
[c] Institute of Chemistry, University of Graz, NAWI Graz, Heinrichstrasse 28, Graz, A-8010 Austria
[d] Department of Organic Chemistry, University of Szeged, Dóm tér 8, Szeged, H-6720 Hungary
[e] Material and Solution Structure Research Group and Interdisciplinary Excellence Centre, Institute of Chemistry, University of Szeged, Aradi Vértanúk tere 1, Szeged, H-6720 Hungary
[f] Department of Applied and Environmental Chemistry, University of Szeged, Rerrich Béla tér 1, Szeged, H-6720 Hungary
[g] MTA-SZTE Reaction Kinetics and Surface Chemistry Research Group, Rerrich Béla tér 1, Szeged, H-6720 Hungary

ARTICLE INFO

Keywords:
Benzylic alcohols
Continuous flow dehydrogenation
Silver-containing hybrid catalyst
Structural characterization

ABSTRACT

In the present contribution, we are reporting our findings on the structure, stability and synthetic applicability of a silver-containing hybrid material, which has recently been introduced by our research groups as a mineralogically-inspired novel heterogeneous catalyst. To determine how silver ions can be fixed into the structure of the catalyst, a set of experiments was designed with modification of the interlayer gallery under hydrothermal conditions. Subsequently, the stability of the material was examined in various solvents under demanding continuous flow conditions with the aim of achieving a clear picture of its applicability in organic syntheses. On the basis of the useful data obtained during the stability tests, a continuous flow methodology was developed for catalytic dehydrogenation of diversely substituted benzylic alcohols. As far as selectivity is concerned the catalyst performed superbly, while the conversions were varied from fair to extremely good.

1. Introduction

In recent years, silver has gained significant importance as catalyst in organic reactions [1–8]. Silver catalysts are environmentally benign and more economical than other commonly used transition metal catalysts, such as gold, palladium and platinum. Thus, silver-catalysed transformations are gaining importance not only in academic research but also in industry. In most cases, silver complexes [9–12] and commercially available silver salts [13–16] are employed as homogeneous catalytic sources. Since the robustness and reusability of such catalysts are extremely beneficial as concerns process simplicity and sustainability, heterogeneous silver catalysts are also known; however, in most cases active silver species, such as nanoparticles, are immobilized *via* weak forces, which often involves inadequate catalyst stability, particularly under demanding reaction conditions [17–20]. Heterogeneous catalysts containing silver play key role not only in organic syntheses but also in environmental applications, such as catalytic elimination of pollutants [21]. Numerous quick and simple methods can be found in the literature for the heterogenization of the transition metal ions as well as nanoparticles [22–28]. Some of them proved to be useful tools to carry out complex organic oxidations or multicomponent reactions [29–33]. Nevertheless, silver-containing heterogeneous catalysts are still less represented than their soluble counterparts [34–36].

Continuous flow reaction technology has become an important tool for the synthetic and medicinal chemistry fields [37–42], and has been extensively investigated to improve the synthesis of active

* Corresponding authors at: MTA-SZTE Stereochemistry Research Group, Hungarian Academy of Sciences, Eötvös u. 6, Szeged, H-6720 Hungary.
** Corresponding author at: Department of Organic Chemistry, University of Szeged, Dóm tér 8, Szeged, H-6720 Hungary.
E-mail addresses: sandor.oetvoes@uni-graz.at (S.B. Ötvös), palinko@chem.u-szeged.hu (I. Pálinkó), fulop@pharm.u-szeged.hu (F. Fülöp).

https://doi.org/10.1016/j.mcat.2020.111263
Received 17 August 2020; Received in revised form 23 September 2020; Accepted 12 October 2020

pharmaceutical ingredients [43–49], nanomaterials [50–52] or other complex substances [53–55]. Transition metal-catalysed reactions under flow chemistry conditions have been shown to have many advantages over traditional batch methods [56–61]. However, such reactions frequently require harsh conditions, such as high temperature and high pressure, and the continuous flow of the reaction medium exert a pronounced mechanical stress for solid materials, which together often contribute to limited applicability and stability of heterogeneous transition metal catalysts in flow reactors [62].

It is well-known that different solvents may exert significant effects on the performance of homogeneous as well as heterogeneous catalysts [63]. Therefore, in the course of a catalytic reaction, it is crucial to choose the appropriate solvent [64,65], and this is especially true for flow conditions to ensure reaction homogeneity and to avoid clogging in reactor channels. One of the most important limitations of heterogeneous materials being employed as catalysts in flow systems is their incompatibility with certain solvents [66]. In these cases, temperature-dependent solvent interactions result in irreversible structural changes, which significantly reduce catalyst robustness and performance. For example, amide type solvents delaminate the layers of layered double hydroxides, which leads to the collapse of catalyst structure and leaching under flow conditions [67].

Recently, we reported on a silver–bismuth hybrid, beyerite-like [68] material (AgBi-HM) with structurally-bound silver catalytic centres, and successfully employed it for heterogeneous catalytic C≡C bond activation to yield organic nitriles directly from terminal alkynes under batch reaction conditions [69]. Although the as-prepared material was completely characterized, the actual position of silver ions in the catalyst lattice remained unresolved. In the present contribution, we report our new findings on the structure of the AgBi-HM, and also on the stability of the material in different solvents under a variety of continuous flow conditions. Finally, aided by the data acquired in elaborate stability tests, we aimed for a simple continuous flow methodology for catalytic dehydrogenation of benzylic alcohols to the corresponding aldehydes as valuable substances; the results are presented herein.

2. Experimental

2.1. General information

All fine chemicals, materials and reagents used were commercially available, and were applied as received without further purification. The benzyl alcohol substrates (with purity of ≥98 %) and the solvents used for catalyst stability experiments and also for dehydrogenation reactions were purchased from Sigma-Aldrich (Merck) and VWR. Analytical thin-layer chromatography was performed on Merck silica gel 60 F254 plates and flash column chromatography on Merck silica gel 60. Compounds were visualized by means of UV or $KMnO_4$. NMR spectra were recorded on a Bruker Avance DRX 500 spectrometer, in $CDCl_3$ as solvent, with TMS as internal standard, at 500.1 and 125 MHz, respectively. GC–MS analyses were performed on a Thermo Scientific Trace 1310 Gas Chromatograph coupled with a Thermo Scientific ISQ QD Single Quadrupole Mass Spectrometer using a ThermoScientific TG-SQC column (15 m × 0.25 mm ID × 0.25 μ film). Measurement parameters were as follows. Column oven temperature: from 50 to 300 °C at 15 °C/min, injection temperature: 240 °C, ion source temperature: 200 °C, electrospray ionization: 70 eV, carrier gas: He at 1.5 mL min^{-1}, injection volume: 2 μL, split ratio: 1:33.3, mass range: 50–500 *m/z*.

2.2. Synthesis and characterization of the AgBi-HM

AgBi-HM was prepared by using the urea hydrolysis method following our previously reported procedure [70]. In this way, the pH could precisely be controlled through the temperature of the co-hydrolysis. In a typical synthesis, the adequate amounts of $AgNO_3$ (3.73 g) and $Bi(NO_3)_3{\cdot}5H_2O$ (5.36 g) were dissolved in 50–50 mL 5 wt% nitric acid. After mixing, urea (7.05 g) dissolved in 100 mL of deionized water was added to the solution and stirred for 72 h at 130 °C. As an alternative way of the synthesis, after addition of the urea solution to the mixture of the required salts, the reaction mixture was placed into an oven for 24 h at 105 °C. The obtained material was next filtrated, washed with aqueous thiosulfate solution, water and ethanol four times, and dried at 60 °C to obtain the final product.

AgBi-HM was fully characterized by means of diverse instrumental techniques as detailed earlier [59]. In the present study, the as-prepared and the treated samples of the material were checked by X-ray diffractometry (XRD), Raman and IR spectroscopies as well as SEM-EDX measurements. Powder XRD patterns were registered in the 2θ = 4°–60° range on a Rigaku Miniflex II instrument using Cu Kα (λ = 1.5418 Å) radiation. FT-IR spectra were measured on a BIO-RAD Digilab Division FTS-65A/896 spectrophotometer with 4 cm^{-1} resolution. 256 scans were collected for each spectrum. The spectra of each sample were recorded with diffuse reflection technique by fixing the incident angle in 45° position. Raman spectra were measured with a Thermo Scientific™ DXR™ Raman microscope at an excitation wavelength of 635 nm applying 10 mW laser power and averaging 20 spectra with an exposure time of 6 s. The actual silver-bismuth molar ratios in the samples before and after treatment were determined by performing SEM-EDX measurements with an S-4700 scanning electron microscope (SEM, Hitachi, Japan) with accelerating voltage of 10–18 kV coupled with a Röntec QX2 energy dispersive microanalytical system.

2.3. Anion-exchange experiments under hydrothermal conditions

For hydrothermal treatment of the AgBi-HM, highly concentrated iodide (c_{NaI} = 4 M), chloride (c_{NaCl} = 4 M) and carbonate (c_{Na2CO3} = 3 M) aqueous solutions were prepared and used. The direct anion-exchange tests were carried out in a Teflon-lined stainless steel autoclave at 120 °C for 2 days. The obtained slurries were filtered, washed with water several times and dried at 80 °C overnight. Treated samples were characterized by XRD, Raman and IR spectroscopies, as well as SEM-EDX measurements.

2.4. Procedure for investigating the solvent compatibility of AgBi-HM under flow conditions

To examine the stability of the as-prepared AgBi-HM, a simple continuous flow set-up was assembled (Fig. 1). The system consisted of an HPLC pump (JASCO PU-2085), a stainless steel cartridge with internal dimensions of 30 × 2.1 mm and a 10-bar backpressure regulator (BPR; IDEX) to enable overheating of the solvents. The column was charged with approximately 50 mg of the AgBi-HM, and was sealed with compatible frits (0.5 μm pore size). Parts of the system were connected with stainless steel capillary tubing (internal diameter 250 μm). The catalyst bed was immersed into an oil bath for heating purposes. In each

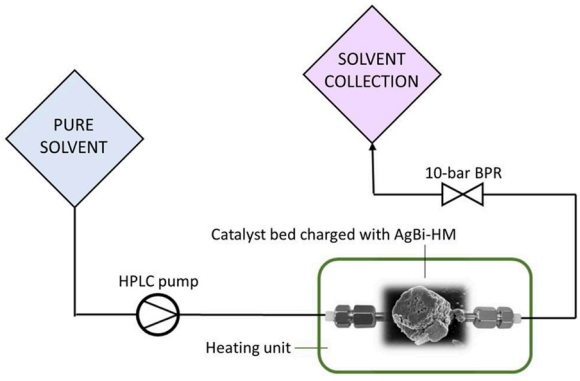

Fig. 1. Experimental setup for the continuous flow experiments.

test, the selected solvent was continuously pumped through the column for 90 min under the appropriate conditions. The treated hybrid material sample was then removed from the cartridge, and was examined by XRD and IR spectroscopy.

2.5. Procedure for AgBi-HM-catalysed alcohol dehydrogenations under flow conditions

The silver-catalysed dehydrogenation reactions were carried out by using the same flow system as the one used for the solvent compatibility tests (Fig. 1). As catalyst bed, a stainless steel cartridge with internal dimensions of 100 × 4.6 mm was used, which encompassed approximately 2 g of AgBi-HM. For each reaction, the corresponding benzyl alcohol (c = 0.075 M) was dissolved in toluene, and the solution was pumped continuously under the selected conditions. In each run, 4 mL of product solution was collected. Between two experiments, the system was washed for 20 min by pumping toluene at a flow rate of 0.5 mL min^{-1}. The crude products were checked by NMR spectroscopy, to determine the conversions and the selectivities. If necessary, column chromatographic purification was carried out with mixture of hexane and EtOAc as eluent. The reaction products were characterized by NMR and MS techniques. The characterization data can be found in the *Supporting Information (SI)* file.

3. Results and discussion

3.1. Indirect proof of the structure of the AgBi-HM

From our earlier investigations [70], it was clear that the AgBi-HM contained Ag(I) and Bi(III) cationic and carbonate anionic components with silver ion as the minor cationic component. The material exhibited layered structure resembling that of a mineral called beyerite ($CaBi_2O_2(CO_3)_2$) [69], which contains Ca(II) ions fixed between $BiO(CO)_3$ layers. In the hybrid material, Bi(III) ions are connected *via* one of the oxygen atoms of the carbonate ions and they are constituents of the layers. At that point, we speculated that Ag(I) ions as minor cationic component are residing among the Bi(III)-containing layers, and are strongly coordinated to the carbonate ions. As concerns the catalytic applicability of the hybrid material, this structural information is of crucial importance. For example, it is essential to know how leaching of the active component can occur, and whether it takes place in a way that the lamellar structure remains intact. On the other hand, the inserted lamellar (Aurivillius) structure may not only be formed by intercalating silver cations among the bismutite layers, but also via incorporating those into the framework of the structure [71]. Accordingly, the removal of silver content without definitive termination of the long-range order of the lamellar structure is only possible from the interlayer-modified bismutite.

To prove the presence or absence of exchangeable interlayer anions of silver species, anion exchange reactions were attempted in the presence of highly concentrated 'entry' anions under hydrothermal conditions. As-prepared AgBi-HM samples were thus treated with concentrated NaI, NaCl or Na_2CO_3 aqueous solutions at 120 °C for 2 days, and the treated samples were compared to the as-prepared one.

As can be seen in Fig. 2, the XRD patterns of the treated samples showed large differences from the as-prepared material. The significant shifts in the characteristic peaks as well as the change in the intensities of the reflections indicated that notable anion exchange took place. Moreover, by finding perfect agreement in the JCPDS (Joint Committee of Powder Diffraction Standards – International Centre for Diffraction Data) database, the produced structures could be undoubtedly identified as bismuth oxyiodide (P(owder)D(iffraction)F(ile) #73-2062) and oxychloride (PDF#06-0249) with tetragonal matlockite crystal phase, which is a layered structure. The framework consists of fluorite-like $[M_2O_2]$ layers sandwiched between double halogen layers upon applying iodide and chloride anions, respectively, as entry anions.

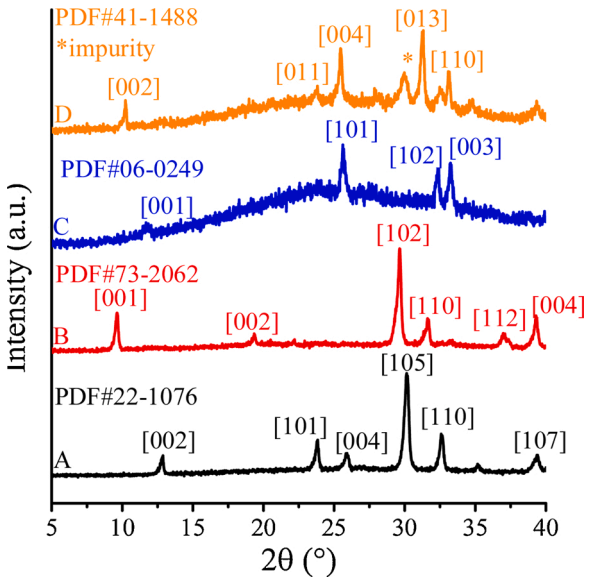

Fig. 2. XRD patterns of AgBi-HM samples: as-prepared material (A), material treated with iodide- (B), chloride- or (C) carbonate-containing solutions (D).

Additionally, by using carbonate as guest anions, pure bismutite (PDF#41-1488) was obtained. It could be assigned to orthorhombic crystal structure similarly to the AgBi-HM. However, because of the theoretical reasons, more expanded interlayer gallery was detected for bismuth subcarbonate without silver ions, which was indicated by the shift of the [002] Bragg reflection into lower 2θ values.

Furthermore, neither the FT-IR nor the Raman spectra of bismuth oxyiodide and oxychloride contained any relevant vibrational bands related to the carbonate species of the raw material (Fig. 3) [72]. In the halogen-containing systems, the broadened stretching vibrations at around 1040 cm^{-1} may be attributed to the Bi–I/Cl band in the BiOI/Cl structure [73]. In addition, the Raman spectra confirmed that the treated materials had oxyiodide/oxychloride structure with the same Raman peaks as in the literature. The characteristic Raman bands at around 180 and 150 cm^{-1} could be associated with A_{1g} internal Bi–Cl stretching and E_g external Bi–Cl stretching modes of bismuth oxychloride upon intercalation of chloride anions [74]. Moreover, two incisive characteristic bands at 160 and 81 cm^{-1} of the iodine-treated samples were assigned to A_{1g} and E_g stretching modes of bismuth oxyiodide [75]. Additionally, by means of SEM-EDX measurements, the loss of the silver cations from the treated structures could also be illustrated (Fig. 4).

These results lead to the conclusion that by performing hydrothermal heat treatment on the Aurivillius structures in the presence of highly concentrated anions, partial or complete anion exchange could be achieved. At the same time, the silver content also diminished. Consequently, it has been proven that silver cations are fixed among the bismutite-like layers of the hybrid material in the form of silver-containing anionic species.

3.2. Investigating the stability and solvent-compatibility of the AgBi-HM under continuous flow conditions

To obtain valuable data on the applicability of the AgBi-HM for organic synthesis in continuous flow mode, the effects of various solvents and reaction conditions on the structure of the material were examined. A simple flow reactor set-up was assembled as detailed in the *Experimental* section. A comprehensive list of solvents was compiled for the stability tests comprising polar, non-polar, protic and aprotic ones. This included CH_2Cl_2, $CHCl_3$, EtOAc, acetone, diethyl ether, MeOH, EtOH, *i*PrOH, H_2O, MeCN, tetrahydrofuran (THF), *N*-methyl-2-

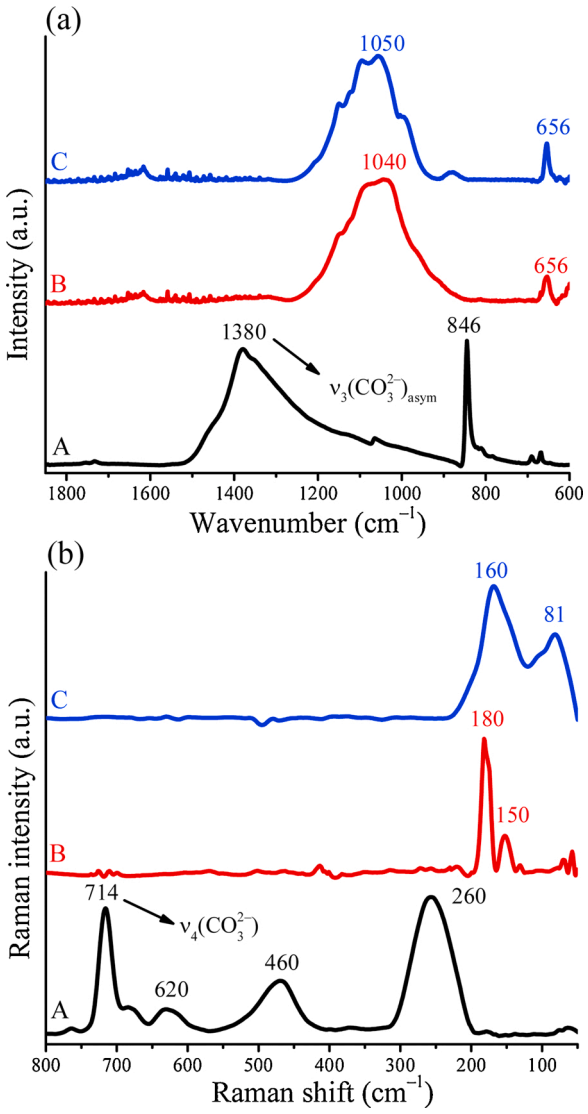

Fig. 3. (a) IR and (b) Raman spectra of AgBi-HM samples: as-prepared material (A), material treated with iodide- (B) or chloride-containing solutions (C).

pyrrolidone (NMP), *n*-hexane, toluene, *N*,*N*-dimethylformamide (DMF), dimethyl sulfoxide (DMSO) and *N*,*N*-dimethylacetamide (DMA). In each test, the appropriate solvent was pumped for 90 min at 0.5 mL min^{-1} flow rate through a catalyst bed encompassing a sample of AgBi-HM. The tests were carried out at 25, 50, 100, 150 and 200 °C as temperatures typically used in catalytic flow reactions. It should be noted that according to TG and DTG measurements, the structure of the hybrid material is thermally stable until 380 °C [70].

The XRD patterns of the treated AgBi-HM samples verified that none of the tested conditions caused collapse or even damage of the structure of the as-prepared material. This was also found for DMF and DMA, which are known as delaminating solvents for certain layered materials [67]. For toluene, DMSO, H_2O, MeCN and EtOAc, the XRD patterns of the treated samples were analogous with that of the as-prepared material at most of the temperatures investigated (Fig. 5, diffractograms B and C as examples). The calculated basal spacings related to the lamellar structures were exactly the same before and after the solvent treatment. In certain solvents, such as acetone, CH_2Cl_2, diethyl ether and alcohols, the XRD patterns were still typical of the beyerite-like hybrid material with basal reflections in the 2θ = 9–38° region, but doubling of characteristic reflections appeared on their diffractograms at different temperatures (Fig. 5, diffractograms D and E as examples). This observation

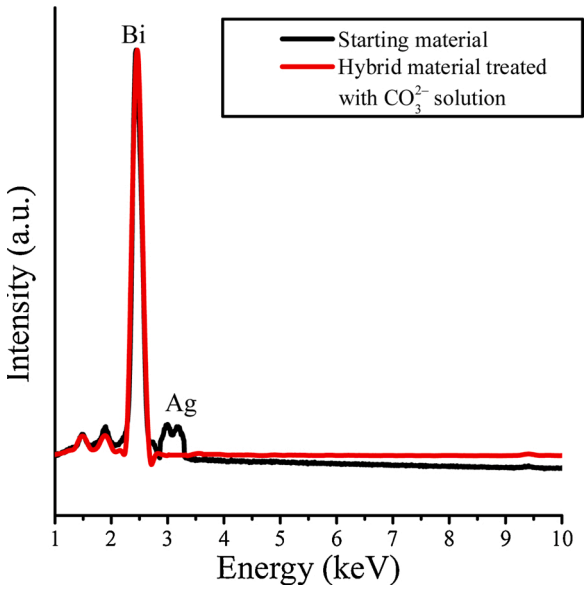

Fig. 4. EDX spectra of the as-prepared AgBi-HM and the one treated with carbonate-containing solution.

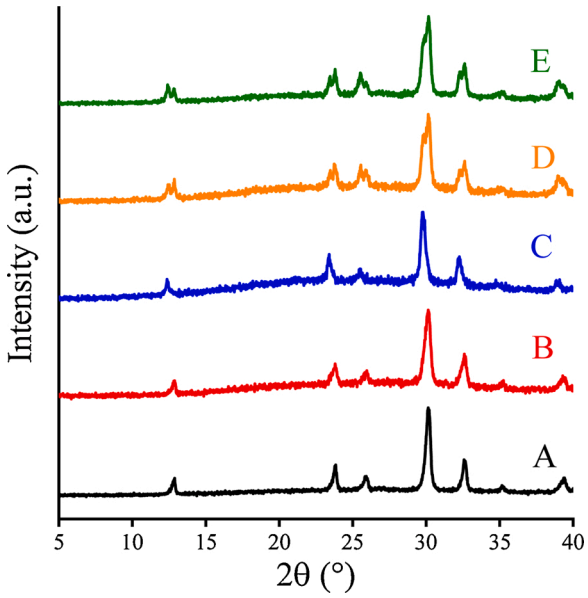

Fig. 5. XRD patterns of AgBi-HM samples: as-prepared material (A), sample treated with toluene at 25 °C (B), sample treated with H_2O at 150 °C (C), sample treated with *i*PrOH at 50 °C (D) and sample treated with diethyl ether at 25 °C (E).

is very similar to the well-known staging effect of lamellar structures [76], and may be explained by partial recrystallization and the formation of a new phase with increased interlayer distances. IR spectra of samples with doubled reflections showed the typical characteristics of the non-treated material, the new absorption bands appeared at around 2900 cm^{-1} can be identified as C—H stretching vibrations of organic solvent traces (Fig. S18) [77]. The results of the stability tests are summarized in Table 1, and the complete collection of diffractograms is presented in the *SI* file.

3.3. Catalytic dehydrogenation of benzylic alcohols under flow conditions

Encouraged by the promising results on the stability of the AgBi-HM

Table 1
Summary of the results of the AgBi-HM stability tests under flow conditions. (A: XRD patterns analogous with that of the as-prepared material, B: doubled characteristic reflections.).

Entry	Solvent	25 °C	50 °C	100 °C	150 °C	200 °C
1	acetone	A	B	B	B	B
2	DMA*	A	A	A	B	B
3	toluene	A	A	A	A	A
4	THF*	A	A	B	B	B
5	DMSO*	A	A	A	A	A
6	$CHCl_3$	B	B	A	A	A
7	*i*PrOH	A	B	B	B	A
8	CH_2Cl_2	B	B	B	B	B
9	MeOH	B	B	B	B	B
10	NMP*	B	B	A	B	A
11	diethyl ether	B	B	B	B	B
12	EtOH	B	B	B	B	A
13	H_2O	B	A	A	A	A
14	MeCN	A	A	A	A	A
15	hexane	B	B	A	A	A
16	DMF*	B	B	A	B	A
17	EtOAc	A	A	A	A	A

* tetrahydrofuran (THF), N-methyl-2-pyrrolidone (NMP), N,N-dimethylformamide (DMF), dimethyl sulfoxide (DMSO), N,N-dimethylacetamide (DMA).

under demanding conditions, we next turned our attention to potential synthetic applications in continuous flow mode. As a consequence of the ubiquity of carbonyl compounds, catalytic oxidation/dehydrogenation of alcohols are of fundamental importance in synthetic organic chemistry and, accordingly, in the fine chemical and pharmaceutical industries [78–82]. Oxidant-free dehydrogenation processes are cleaner, more atom-efficient, and due to the lack of over-oxidation, generally more selective than catalytic oxidations [83–85]. However, such reactions typically require harsh conditions, and hence pose a significant synthetic challenge. In fact, besides well-established industrial processes for gas-phase alcohol dehydrogenations [86,87], liquid-phase catalytic methodologies are quite limited, and often suffer from significant drawbacks, such as low activity, limited substrate scope and the necessity of various additives [88–91]. Inspired by these factors, we selected catalytic dehydrogenation of benzylic alcohols as a benchmark to evaluate the synthetic capability of the AgBi-HM catalyst under demanding flow conditions.

To investigate the effects of reaction conditions on the catalytic dehydrogenation, 4-methylbenzyl alcohol was selected as a model substrate. Initially, the AgBi-HM catalyst was tested under batch conditions and, in parallel, another reaction was performed under the same conditions using $AgNO_3$ as catalyst (Scheme 1). After stirring for 24 h in refluxing toluene (110 °C), 62 % conversion was detected with the hybrid material, whereas $AgNO_3$ gave only 15 % conversion (selectivity was 100 % in both reactions). No conversion was detected without the presence of catalyst. The enhanced activity of the catalyst – compared to silver nitrate salt – may be assigned to the promoter roles of the bismuth centres and the oxide surface. A possible reaction mechanism was suggested accordingly (Scheme S1). Moreover, in our opinion, the exclusive selectivity is the contribution not only of Ag(I) centres but the shape-selective effect of the layered structure.

The promising preliminary results encouraged us to explore the reaction further under continuous flow conditions using a simple fixed-bed system as shown in Fig. 1. Considering that the AgBi-HM was proven to be compatible with wide variety of solvents even at high temperatures (Table 1), extensive solvent screening was carried out at 180 °C (Table 2). The reaction outcome proved to be strongly dependent on the solvent applied. In acetone, CH_2Cl_2, EtOAc and MeCN, conversions of 20–46 % were detected; however, selectivity was very low (entries 1–4). Contrarily, in DMSO, MeOH, THF or toluene, selective aldehyde formation was observed (entries 5–8). The highest conversion was achieved in toluene (92 %, entry 8), which was therefore chosen as solvent for further parameter optimization.

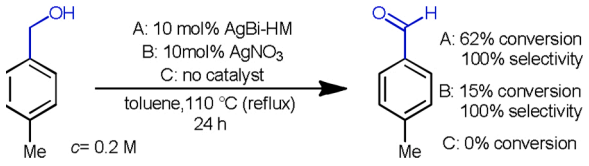

Scheme 1. Catalytic dehydrogenation of 4-methylbenzyl alcohol under batch conditions.

The reaction temperature was found to have significant role on the conversion and the selectivity (Fig. 6a). For example, at 100 °C, conversion of merely 13 % occurred, which was improved remarkably upon gradual increase of the temperature. Gratifyingly, at 180 °C, 92 % conversion and 100 % selectivity were observed. However, further increase to 200 °C triggered the benzylation of toluene with the substrate as competing side reaction, and thus provoked a momentous decrease in selectivity to 62 % (besides a marginal increase in conversion). Such benzylations are known from the literature, and can be accessed in the presence of various metal catalysts typically at higher temperatures [92, 93]. The residence time also had significant effects on the reaction outcome. Upon decreasing the flow rate from 150 μL min^{-1}, the conversion gradually improved from 64 % until it finally reached 100 % at 20 μL min^{-1} (Fig. 6b), which corresponded to a residence time of approximately 75 min. However, at 20 μL min^{-1} flow rate, the competing benzylation appeared as side reaction, and reduced the selectivity to 56 %. As optimum flow rate, 30 μL min^{-1} was selected (corresponding to 50 min residence time), which ensured an excellent conversion of 92 % and fully selective aldehyde formation. The effects of substrate concentration were also examined (Table S1), and 0.075 M was found to be the best as higher concentrations led to lower selectivity due to side product formation.

Based on the findings of the parameter optimization, the reaction was operated most efficiently at 30 μL min^{-1} flow rate and 180 °C reaction temperature with a substrate concentration of 0.075 M. With these conditions in hand, we finally set out to investigate the substrate scope of the process (Table 3). Excellent conversions were found for substituted benzyl alcohol derivatives containing methyl, methoxy, bromo and nitro groups in the *para* position. The reactions also worked well with meta-substituted benzyl alcohols, and furnished conversions in the range of 36–82 %. The multisubstituted 3-methyl-4-nitrobenzyl alcohol gave an acceptable conversion of 40 %. Dehydrogenation of 2-bromobenzyl alcohol was also attempted, but due to the significant steric hindrance generated by the *ortho* bromo moiety, the conversion of the substrate was merely 18 %. It is remarkable that in all reactions, fully selective aldehyde formation was observed, side products were not detected.

Table 2
Investigating the effects of various solvents on the dehydrogenation reaction of 4-methylbenzyl alcohol under continuous flow conditions.

Entry	Solvent	Conv.[a] (%)	Sel.[a] (%)
			
1	acetone	20	traces
2	CH_2Cl_2	36	traces
3	EtOAc	46	25
4	MeCN	27	40
5	DMSO	8	100
6	MeOH	4	100
7	THF	22	100
8	toluene	92	100

[a] Determined by ^{1}H NMR analysis of the crude product.

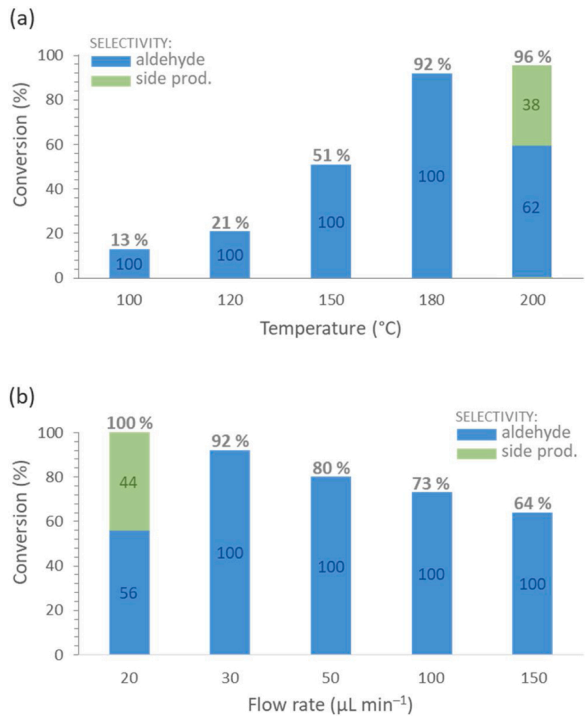

Fig. 6. Investigating the effects of temperature (a) and flow rate (b) on the AgBi-HM-catalysed dehydrogenation of 4-methylbenzyl alcohol under continuous flow conditions. (Reaction conditions: $c = 0.075$ M, toluene as solvent, 30 µL min^{-1} flow rate for the temperature study, 180 °C temperature for the flow rate study.).

Table 3
AgBi-HM-catalyzed dehydrogenation of diversely substituted benzyl alcohols under continuous flow conditions.

Entry	Substrate	Conv.[a] (%)	Sel.[a] (%)
	180 °C, 30 µL min^{-1}, toluene; AgBi-HM; c= 0.075 M		
1	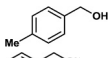	92	100
2	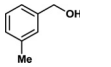	82	100
3	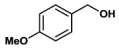	95	100
4	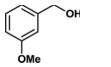	36	100
5	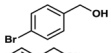	70	100
6	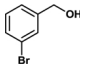	59	100
7	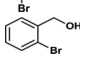	18	100
8	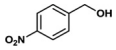	73	100
9	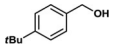	43	100
10	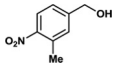	40	100

[a] Determined by ^{1}H NMR analysis of the crude product.

4. Conclusions

By strategic anion-exchange reactions under hydrothermal conditions, the modification of the interlayer gallery of the AgBi-HM was successfully achieved, which indirectly proved that silver cations were fixed among the layers of the material as silver-containing anionic species. The stability of the material was investigated in a wide variety of organic solvents under continuous flow conditions to aid potential synthetic applications. It was found that none of the tested solvents resulted in the collapse or even damage of the structure of the material, even at temperatures as high as 200 °C. As proof of concept, a novel continuous flow protocol was established for catalytic dehydrogenation of benzylic alcohols using the hybrid material as catalyst. The effects of reaction temperature, residence time, substrate concentration and various solvents were explored to achieve high conversions and selective aldehyde formation without the need for any additives. The scope and applicability of the flow protocol was also demonstrated.

CRediT authorship contribution statement

Rebeka Mészáros: Investigation, Data curation, Writing - original draft. **Sándor B. Ötvös:** Conceptualization, Supervision, Writing - review & editing. **Gábor Varga:** Investigation, Data curation. **Éva Böszörményi:** Investigation. **Marianna Kocsis:** Investigation. **Krisztina Karádi:** Investigation. **Zoltán Kónya:** Methodology. **Ákos Kukovecz:** Methodology. **István Pálinkó:** Conceptualization, Supervision, Validation, Writing - review & editing. **Ferenc Fülöp:** Supervision, Resources.

Declaration of Competing Interest

The authors report no competing interest.

Acknowledgements

Financial support was obtained from the ÚNKP-19-3 New National Excellence Program of the Ministry for Innovation and Technology (Hungary). SBÖ acknowledges the Premium Post Doctorate Research Program of the Hungarian Academy of Sciences. All these supports are highly appreciated.

Appendix A. Supplementary data

Supplementary material related to this article can be found, in the online version, at doi:https://doi.org/10.1016/j.mcat.2020.111263.

References

[1] Z. Chen, N. Ren, X. Ma, J. Nie, F.-G. Zhang, J.-A. Ma, Silver-catalyzed [3 + 3] dipolar cycloaddition of trifluorodiazoethane and glycine imines: access to highly functionalized trifluoromethyl-substituted triazines and pyridines, ACS Catal. 9 (2019) 4600–4608.
[2] J. George, H.Y. Kim, K. Oh, Silver-catalyzed asymmetric desymmetrization of cyclopentenediones via [3 + 2] cycloaddition with α-substituted isocyanoacetates, Org. Lett. 20 (2018) 2249–2252.
[3] A.K. Clarke, J.M. Lynam, R.J.K. Taylor, W.P. Unsworth, "Back-to-Front" indole synthesis using silver(I) catalysis: unexpected C-3 pyrrole activation mode supported by DFT, ACS Catal. 8 (2018) 6844–6850.
[4] Z.-Z. Zhou, M. Liu, L. Lv, C.-J. Li, Silver(I)-catalyzed widely applicable aerobic 1,2-diol oxidative cleavage, Angew. Chem. Int. Ed. 57 (2018) 2616–2620.
[5] Y. Ning, Q. Ji, P. Liao, E.A. Anderson, X. Bi, Silver-catalyzed stereoselective aminosulfonylation of alkynes, Angew. Chem. Int. Ed. 56 (2017) 13805–13808.
[6] K. Sekine, T. Yamada, Silver-catalyzed carboxylation, Chem. Soc. Rev. 45 (2016) 4524–4532.
[7] H. Pellissier, Enantioselective silver-catalyzed transformations, Chem. Rev. 116 (2016) 14868–14917.
[8] V.K.-Y. Lo, A.O.-Y. Chan, C.-M. Che, Gold and silver catalysis: from organic transformation to bioconjugation, Org. Biomol. Chem. 13 (2015) 6667–6680.
[9] A. Yanagisawa, N. Yang, K. Bamba, Asymmetric allylation of carbonyl compounds catalyzed by a chiral phosphine–silver complex, Eur. J. Org. Chem. (2017) 6614–6618.
[10] A. Koizumi, M. Harada, R. Haraguchi, S.-I. Fukuzawa, Chiral silver complex-catalyzed diastereoselective and enantioselective Michael addition of 1-Pyrroline-5-carboxylates to α-enones, J. Org. Chem. 82 (2017) 8927–8932.
[11] S. Ghorai, D. Lee, Aryne formation via the hexadehydro Diels-Alder reaction and their Ritter-type transformations catalyzed by a cationic silver complex, Tetrahedron 73 (2017) 4062–4069.

[12] A. Yanagisawa, Y. Lin, A. Takeishi, K. Yoshida, Enantioselective nitroso aldol reaction catalyzed by a chiral phosphine–silver complex, Eur. J. Org. Chem. (2016) 5355–5359.
[13] R.J. Scamp, B. Scheffer, J.M. Schomaker, Regioselective differentiation of vicinal methylene C–H bonds enabled by silver-catalysed nitrene transfer, Chem.Commun. 55 (2019) 7362–7365.
[14] M. Dell'Acqua, V. Pirovano, S. Peroni, G. Tseberlidis, D. Nava, E. Rossi, G. Abbiati, Silver-catalysed domino approach to 1,3-dicarbo-substituted isochromenes, Eur. J. Org. Chem. (2017) 1425–1433.
[15] S. Guo, F. Cong, R. Guo, L. Wang, P. Tang, Asymmetric silver-catalysed intermolecular bromotrifluoromethoxylation of alkenes with a new trifluoromethoxylation reagent, Nat. Chem. 9 (2017) 546–551.
[16] X. Zhou, C. Huang, Y. Zeng, J. Xiong, Y. Xiao, J. Zhang, Silver-catalysed tandem hydroamination and cyclization of 2-trifluoromethyl-1,3-enynes with primary amines: modular entry to 4-trifluoromethyl-3-pyrrolines, Chem. Commun. 53 (2017) 1084–1087.
[17] J. An, G. Sun, H. Xia, Aerobic oxidation of 5-hydroxymethylfurfural to high-yield 5-hydroxymethyl-2-furancarboxylic acid by poly(vinylpyrrolidone)-capped Ag nanoparticle catalysts, ACS Sustainable Chem. Eng. 7 (2019) 6696–6706.
[18] W.-J. Chen, B.-H. Cheng, Q.-T. Sun, H. Jiang, Preparation of MOF confined Ag nanoparticles for the highly active, size selective hydrogenation of olefins, ChemCatChem 10 (2018) 3659–3665.
[19] B. Ballarin, D. Barreca, E. Boanini, M.C. Cassani, P. Dambruoso, A. Massi, A. Mignani, D. Nanni, C. Parise, A. Zaghi, Supported gold nanoparticles for alcohols oxidation in continuous-flow heterogeneous systems, ACS Sustainable Chem. Eng. 5 (2017) 4746–4756.
[20] X.-Y. Dong, Z.-W. Gao, K.-F. Yang, W.-Q. Zhang, L.-W. Xu, Nanosilver as a new generation of silver catalysts in organic transformations for efficient synthesis of fine chemicals, Catal. Sci. Technol. 5 (2015) 2554–2574.
[21] C. Wen, A. Yin, W.-L. Dai, Recent advances in silver-based heterogeneous catalysts for green chemistry processes, Appl. Catal. B 160-161 (2014) 730–741.
[22] M.S. Esmaeili, Z. Varzi, R. Eivazzadeh-Keihan, A. Maleki, H. Ghafuri, Design and development of natural and biocompatible raffinose-Cu_2O magnetic nanoparticles as a heterogeneous nanocatalyst for the selective oxidation of alcohols, Mol. Catal. 492 (111037) (2020) 1–12.
[23] R. Eivazzadeh-Keihan, F. Radinekiyan, A. Maleki, M.S. Bani, Z. Hajizadeh, S. Asgharnasl, A novel biocompatible core-shell magnetic nanocomposite based on cross-linked chitosan hydrogels for in vitro hyperthermia of cancer therapy, Int. J. Biol. Macromol. 140 (2019) 407–414.
[24] J. Rahimi, R. Taheri-Ledari, M. Niksefat, A. Maleki, Enhanced reduction of nitrobenzene derivatives: effective strategy executed by Fe_3O_4/PVA-10% Ag as a versatile hybrid nanocatalyst, Catal. Commun. 134 (105850) (2020) 1–6.
[25] A. Maleki, K. Valadi, S. Gharibi, R. Taheri-Ledari, Convenient and fast synthesis of various chromene pharmaceuticals assisted by highly porous volcanic micro-powder with nanoscale diameter porosity, Res. Chem. Intermed. 46 (2020) 4113–4128.
[26] A. Maleki, T. Kari, Novel leaking-free, green, double core/shell, palladium-loaded magnetic heterogeneous nanocatalyst for selective aerobic oxidation, Catal. Lett. 148 (2018) 2929–2934.
[27] M. Azizi, A. Maleki, F. Hakimpoor, Solvent, metal and halogen-free synthesis of sulfoxides by using a recoverable heterogeneous urea-hydrogen peroxide silica-based oxidative catalytic system, Catal. Commun. 100 (2017) 62–65.
[28] R. Firouzi-Haji, A. Maleki, L-proline-functionalized Fe_3O_4 nanoparticles as an efficient nanomagnetic organocatalyst for highly stereoselective one-pot two-step tandem synthesis of substituted cyclopropanes, ChemistrySelect 4 (2019) 853–857.
[29] Z. Hajizadeh, A. Maleki, Poly (ethylene imine)-modified magnetic halloysite nanotubes: a novel, efficient and recyclable catalyst for the synthesis of dihydropyrano [2, 3-c] pyrazole derivatives, Mol. Catal. 460 (2018) 87–93.
[30] A. Maleki, M. Rabbani, S. Shahrokh, Preparation and characterization of a silica-based magnetic nanocomposite and its application as a recoverable catalyst for the one-pot multicomponent synthesis of quinazolinone derivatives, Appl. Organomet. Chem. 29 (2015) 809–814.
[31] A. Maleki, Green oxidation protocol: selective conversions of alcohols and alkenes to aldehydes, ketones and epoxides by using a new multiwall carbon nanotube-based hybrid nanocatalyst via ultrasound irradiation, Ultrason. Sonochem. 40 (2018) 460–464.
[32] A. Maleki, R. Rahimi, S. Maleki, Efficient oxidation and epoxidation using a chromium (VI)-based magnetic nanocomposite, Environ. Chem. Lett. 14 (2016) 195–199.
[33] A. Shaabani, A. Maleki, Green and efficient synthesis of quinoxaline derivatives via ceric ammonium nitrate promoted and in situ aerobic oxidation of α-hydroxy ketones and α-keto oximes in aqueous media, Chem. Pharm. Bull. 56 (2008) 79–81.
[34] A. Zuliani, P. Ranjan, R. Luque, E.V. Van der Eycken, Heterogeneously catalyzed synthesis of imidazolones via cycloisomerizations of propargylic ureas using Ag and Au/Al SBA-15 systems, ACS Sustainable Chem. Eng. 7 (2019) 5568–5575.
[35] E. Plessers, J.E. van den Reijen, P.E. de Jongh, K.P. de Jong, M.B.J. Roeffaers, Origin and abatement of heterogeneity at the support granule scale of silver on silica catalysts, ChemCatChem 9 (2017) 4562–4569.
[36] Z. Zhou, C. He, L. Yang, Y. Wang, T. Liu, C. Duan, Alkyne activation by a porous silver coordination polymer for heterogeneous catalysis of carbon dioxide cycloaddition, ACS Catal. 7 (2017) 2248–2256.
[37] A.R. Bogdan, A.W. Dombrowski, Emerging trends in flow chemistry and applications to the pharmaceutical industry, J. Med. Chem. 62 (2019) 6422–6468.
[38] L. Rogers, K.F. Jensen, Continuous manufacturing – the green chemistry promise? Green Chem. 21 (2019) 3481–3498.
[39] R. Gerardy, N. Emmanuel, T. Toupy, V.-E. Kassin, N.N. Tshibalonza, M. Schmitz, J.-C.M. Monbaliu, Continuous flow organic chemistry: successes and pitfalls at the interface with current societal challenges, Eur. J. Org. Chem. (2018) 2301–2351.
[40] M.B. Plutschack, B. Pieber, K. Gilmore, P.H. Seeberger, The hitchhiker's guide to flow chemistry, Chem. Rev. 117 (2017) 11796–11893.
[41] R. Porta, M. Benaglia, A. Puglisi, Flow chemistry: recent developments in the synthesis of pharmaceutical products, Org. Process Res. Dev. 20 (2016) 2–25.
[42] I.M. Mándity, S.B. Ötvös, F. Fülöp, Strategic application of residence-time control in continuous-flow reactors, ChemistryOpen 4 (2015) 212–223.
[43] S.B. Ötvös, M.A. Pericàs, C.O. Kappe, Multigram-scale flow synthesis of the chiral key intermediate of (−)-paroxetine enabled by solvent-free heterogeneous organocatalysis, Chem. Sci. 10 (2019) 11141–11146.
[44] V.-E.H. Kassin, R. Gerardy, T. Toupy, D. Collin, E. Salvadeo, F. Toussaint, K. van Hecke, J.-C.M. Monbaliu, Expedient preparation of active pharmaceutical ingredient ketamine under sustainable continuous flow conditions, Green Chem. 21 (2019) 2952–2966.
[45] R.E. Ziegler, B.K. Desai, J.-A. Jee, B.F. Gupton, T.D. Roper, T.F. Jamison, 7-step flow synthesis of the HIV integrase inhibitor Dolutegravir, Angew. Chem. Int. Ed. 57 (2018) 7181–7185.
[46] H. Ishitani, K. Kanai, Y. Saito, T. Tsubogo, S. Kobayashi, Synthesis of (±)-Pregabalin by utilizing a three-step sequential-flow system with heterogeneous catalysts, Eur. J. Org. Chem. (2017) 6491–6494.
[47] M.O. Kitching, O.E. Dixon, M. Baumann, I.R. Baxendale, Flow-assisted synthesis: a key fragment of SR 142948A, Eur. J. Org. Chem. (2017) 6540–6553.
[48] S. Borukhova, T. Nöel, V. Hessel, Continuous-flow multistep synthesis of Cinnarizine, Cyclizine, and a Buclizine derivative from bulk alcohols, ChemSusChem 9 (2016) 67–74.
[49] B. Gutmann, D. Cantillo, C.O. Kappe, Continuous-flow technology—a tool for the safe manufacturing of active pharmaceutical ingredients, Angew. Chem. Int. Ed. 54 (2015) 6688–6728.
[50] F.J. Martin-Martinez, K. Jin, D. López Barreiro, M.J. Buehler, The rise of hierarchical nanostructured materials from renewable sources: learning from nature, ACS Nano 12 (2018) 7425–7433.
[51] M.P. Tsang, G. Philippot, C. Aymonier, G. Sonnemann, Supercritical fluid flow synthesis to support sustainable production of engineered nanomaterials: case study of titanium dioxide, ACS Sustainable Chem. Eng. 6 (2018) 5142–5151.
[52] J.J. Pagano, T. Bánsági Jr., O. Steinbock, Bubble-templated and flow-controlled synthesis of macroscopic silica tubes supporting zinc oxide nanostructures, Angew. Chem. Int. Ed. 47 (2008) 9900–9903.
[53] S. Fuse, Y. Otake, H. Nakamura, Peptide synthesis utilizing micro-flow technology, Chem. Asian J. 13 (2018) 3818–3832.
[54] J. Britton, C.L. Raston, Multi-step continuous-flow synthesis, Chem. Soc. Rev. 46 (2017) 1250–1271.
[55] S.B. Ötvös, F. Fülöp, Flow chemistry as a versatile tool for the synthesis of triazoles, Catal. Sci. Technol. 5 (2015) 4926–4941.
[56] J.C. Pastre, D.L. Browne, S.V. Ley, Flow chemistry syntheses of natural products, Chem. Soc. Rev. 42 (2013) 8849–8869.
[57] Y. Deng, X.-J. Wei, X. Wang, Y. Sun, T. Noël, Iron-catalyzed cross-coupling of alkynyl and styrenyl chlorides with alkyl Grignard reagents in batch and flow, Chem. Eur. J. 25 (2019) 14532–14535.
[58] F. Ferlin, P.M. Luque Navarro, Y. Gu, D. Lanari, L. Vaccaro, Waste minimized synthesis of pharmaceutically active compounds via heterogeneous manganese catalysed C–H oxidation in flow, Green Chem. 22 (2020) 397–403.
[59] L.J. Durndell, M.A. Isaacs, C. Li, C.M.A. Parlett, K. Wilson, A.F. Lee, Cascade aerobic selective oxidation over contiguous dual-catalyst beds in continuous flow, ACS Catal. 9 (2019) 5345–5352.
[60] S.B. Ötvös, Á. Georgiádes, R. Mészáros, K. Kis, I. Pálinkó, F. Fülöp, Continuous-flow oxidative homocouplings without auxiliary substances: exploiting a solid base catalyst, J. Catal. 348 (2017) 90–99.
[61] D.C. Crowley, D. Lynch, A.R. Maguire, Copper-mediated, heterogeneous, enantioselective intramolecular buchner reactions of α-diazoketones using continuous flow processing, J. Org. Chem. 83 (2018) 3794–3805.
[62] T. Noel, S.L. Buchwald, Cross-coupling in flow, Chem. Soc. Rev. 40 (2011) 5010–5029.
[63] D. Cantillo, C.O. Kappe, Immobilized transition metals as catalysts for cross-couplings in continuous flow—a critical assessment of the reaction mechanism and metal leaching, ChemCatChem 6 (2014) 3286–3305.
[64] N. Yan, C. Xiao, Y. Kou, Transition metal nanoparticle catalysis in green solvent, Coord. Chem. Rev. 254 (2010) 1179–1218.
[65] L. Vaccaro, M. Curini, F. Ferlin, D. Lanari, A. Marrocchi, O. Piermatti, V. Trombettoni, Definition of green synthetic tools based on safer reaction media, heterogeneous catalysis, and flow technology, Pure Appl. Chem. 90 (2018) 21–33.
[66] D. Prat, A. Wells, J. Hayler, H. Sneddon, C.R. McElroy, S. Abou-Shehada, P.J. Dunn, CHEM21 selection guide of classical- and less classical-solvents, Green Chem. 18 (2016) 288–296.
[67] R. Mészáros, S.B. Ötvös, Z. Kónya, Á. Kukovecz, P. Sipos, F. Fülöp, I. Pálinkó, Potential solvents in coupling reactions catalyzed by Cu(II)Fe(III)-layered double hydroxide in a continuous-flow reactor, React. Kinet. Mech. Cat. 121 (2017) 345–351.
[68] S.B. Ötvös, I. Pálinkó, F. Fülöp, Catalytic use of layered materials for fine chemical syntheses, Catal. Sci. Technol. 9 (2019) 47–60.
[69] V. Malik, M. Pokhriyal, S. Uma, Single step hydrothermal synthesis of beyerite, $CaBi_2O_2(CO_3)_2$ for the fabrication of UV-visible light photocatalyst BiOI/$CaBi_2O_2(CO_3)_2$, RSC Adv. 6 (2016) 38252–38262.
[70] S.B. Ötvös, R. Mészáros, G. Varga, M. Kocsis, Z. Kónya, Á. Kukovecz, P. Pusztai, P. Sipos, I. Pálinkó, F. Fülöp, A mineralogically-inspired silver–bismuth hybrid

material: an efficient heterogeneous catalyst for the direct synthesis of nitriles from terminal alkynes, Green Chem. 20 (2018) 1007–1019.
[71] S. Sun, Y. Huang, G. Wang, J. Wang, Z. Fu, R. Peng, R.J. Knize, Y. Lu, Nanoscale structural modulation and enhanced room-temperature multiferroic properties, Nanoscale 6 (2014) 13494–13500.
[72] G. Zhao, Y. Tian, H. Fan, J. Zhang, L.J. Hu, Properties and structures of Bi_2O_3–B_2O_3–TeO_2 glass, J. Mater. Sci. Technol. 29 (2013) 209–214.
[73] L. Li, M. Zhang, Z. Zhao, B. Sun, X. Zhang, Visible/near-IR-light-driven TNFePc/BiOCl organic–inorganic heterostructures with enhanced photocatalytic activity, Dalton Trans. 45 (2016) 9497–9505.
[74] Y. Myung, J. Choi, F. Wu, S. Banerjee, E.H. Majzoub, J. Jin, S.U. Son, P.V. Braun, P. Banerjee, Cationically substituted $Bi_{0.7}Fe_{0.3}OCl$ nanosheets as Li ion battery anodes, ACS Appl. Mater. Interfaces 9 (2017) 14187–14196.
[75] H. Li, Z. Yang, J. Zhang, Y. Huang, H. Ji, Y. Tong, Indium doped BiOI nanosheets: preparation, characterization and photocatalytic degradation activity, Appl. Surf. Sci. 423 (2017) 1188–1197.
[76] K.K. Bardhan, G. Kirczenow, G. Jackle, J.C. Irwin, Staging structures of the intercalation compounds Ag_xTiS_2, Phys. Rev. B 33 (1986) 4149–4159.
[77] H. Masood, R. Yunus, T.S. Choong, U. Rashid, Y.H.T. Yap, Synthesis and characterization of calcium methoxide as heterogeneous catalyst for trimethylolpropane esters conversion reaction, Appl. Catal. A 425 (2012) 184–190.
[78] V.V. Torbina, A.A. Vodyankin, S. Ten, G.V. Mamontov, M.A. Salaev, V.I. Sobolev, O.V. Vodyankina, Ag-based catalysts in heterogeneous selective oxidation of alcohols: a review, Catalysts 8 (2018) 447.
[79] C. Parmeggiani, C. Matassinia, F. Cardona, A step forward towards sustainable aerobic alcohol oxidation: new and revised catalysts based on transition metals on solid supports, Green Chem. 19 (2017) 2030–2050.
[80] J.K. Mobley, M. Crocker, Catalytic oxidation of alcohols to carbonyl compounds over hydrotalcite and hydrotalcite-supported catalysts, RSC Adv. 5 (2015) 65780–65797.
[81] R. Ciriminna, V. Pandarus, F. Béland, Y.-J. Xu, M. Pagliaro, Heterogeneously catalyzed alcohol oxidation for the fine chemical industry, Org. Process Res. Dev. 19 (2015) 1554–1558.
[82] S.E. Davis, M.S. Ide, R.J. Davis, Selective oxidation of alcohols and aldehydes over supported metal nanoparticles, Green Chem. 15 (2013) 17–45.
[83] J. Zheng, J. Qu, H. Lin, Q. Zhang, X. Yuan, Y. Yang, Y. Yuan, Surface composition control of the binary Au–Ag catalyst for enhanced oxidant-free dehydrogenation, ACS Catal. 6 (2016) 6662–6669.
[84] K. Kon, S.M.A.H. Siddiki, K. Shimizu, Size- and support-dependent Pt nanocluster catalysis for oxidant-free dehydrogenation of alcohols, J. Catal. 304 (2013) 63–71.
[85] T. Mitsudome, Y. Mikami, H. Funai, T. Mizugaki, K. Jitsukawa, K. Kaneda, Oxidant-free alcohol dehydrogenation using a reusable hydrotalcite-supported silver nanoparticle catalyst, Angew. Chem. Int. Ed. 47 (2008) 138–141.
[86] F. Liu, H. Wang, A. Sapi, H. Tatsumi, D. Zherebetskyy, H.-L. Han, L.M. Carl, G. A. Somorjai, Molecular orientations change reaction kinetics and mechanism: a review on catalytic alcohol oxidation in gas phase and liquid phase on size-controlled Pt nanoparticles, Catalysts 8 (2018) 226.
[87] J.V. Ochoa, F. Cavani, Transition Metal Catalysis in Aerobic Alcohol Oxidation, The Royal Society of Chemistry, 2015, pp. 203–230.
[88] D.K. Kurhe, T.A. Fernandes, T.S. Deore, R.V. Jayaram, Oxidant free dehydrogenation of alcohols using chitosan/polyacrylamide entrapped Ag nanoparticles, RSC Adv. 5 (2015) 46443–46447.
[89] A. Bayat, M. Shakourian-Fard, N. Ehyaei, M. Mahmoodi Hashemi, Silver nanoparticles supported on silica-coated ferrite as magnetic and reusable catalysts for oxidant-free alcohol dehydrogenation, RSC Adv. 5 (2015) 22503–22509.
[90] V.L. Sushkevich, I.I. Ivanova, E. Taarning, Mechanistic study of ethanol dehydrogenation over silica-supported silver, ChemCatChem 5 (2013) 2367–2373.
[91] K. Shimizu, K. Sugino, K. Sawabe, A. Satsuma, Oxidant-free dehydrogenation of alcohols heterogeneously catalyzed by cooperation of silver clusters and acid–base sites on alumina, Chem. Eur. J. 15 (2009) 2341–2351.
[92] A.K. Maity, P.N. Chatterjee, S. Roy, Multimetallic Ir–Sn_3-catalyzed substitution reaction of π-activated alcohols with carbon and heteroatom nucleophiles, Tetrahedron 69 (2013) 942–956.
[93] J. Choudhury, S. Podder, S. Roy, Cooperative Friedel−crafts catalysis in heterobimetallic regime: alkylation of aromatics by π-activated alcohols, J. Am. Chem. Soc. 127 (2005) 6162–6163.